

Robust Quantum Griffiths Singularity at above 1.5 Kelvin in Nitride Thin Films

Xiaoni Wang,^{1,2} Lijie Wang,³ Yixin Liu,^{1,2} Fan Chen,^{1,2} Wanpeng Gao,^{1,2} Yu Wu,¹ Zulei Xu,^{1,2}
Wei Peng,^{1,2} Zhen Wang,^{1,2} Zengfeng Di,^{1,2} Wei Li,^{3,*} Gang Mu,^{1,2,†} and Zhirong Lin^{1,2,‡}

¹*State Key Laboratory of Functional Materials for Informatics,
Shanghai Institute of Microsystem and Information Technology,
Chinese Academy of Sciences, Shanghai 200050, China*

²*University of Chinese Academy of Science, Beijing 100049, China*

³*Department of Physics and State Key Laboratory of Surface Physics, Fudan University, Shanghai 200433, China*

Quantum Griffiths singularity (QGS), which is closely correlated with the quenched disorder, is characterized by the divergence of the dynamical critical exponent and the presence of activated scaling behavior. Typically such a quantum phenomenon is rather rare and only observed in extremely low temperatures. Here we report the experimental observation of a robust QGS in nitride thin films, NbN, which survives in a rather high temperature range. The electrical transport properties were measured under the magnetic field up to 12 T. The field induced superconductor-metal transitions were observed with the continuously changed transition points with the decrease of temperature. The dynamical critical exponent based on the conventional power-law scaling reveals a divergent trend when approaching the low temperature limit. Moreover, the temperature and field dependence of sheet resistance can be described by the activated scaling analysis in the temperature region up to $1.6 \text{ K} \leq T \leq 4.0 \text{ K}$. We argue that the robustness of QGS in the present system originates from the Pauli paramagnetic effect due to the strong coupling between the magnetic field and the spin degree of freedom.

PACS numbers: 74.70.-b, 74.25.F-, 73.43.Nq

1 Introduction

The phase transition between different ground states, which is accompanied by quantum rather than thermal fluctuations, is called the quantum transition [1, 2]. For example, the superconductor-insulator transition (SIT) is typically driven by disorder, magnetic field (B), or carrier concentration [3–8]. Such a quantum transition can have a significant influence on the physical performance in finite temperatures in terms of the quantum fluctuations. In the conventional scenes, only one critical transition point exists and the temperature dependent resistance R near the SIT point can be described by a power-law scaling determined by the critical exponents (z , ν) and the distance from the critical point [9–13]. Recently, it was reported that, in the two-dimensional (2D) or quasi-2D systems with quenched disorder, a new type of superconductor-metal transition (SMT) emerges. In these systems, the crossing point in the $R(B)$ curves can realize a systematic variation with temperature and effective critical exponents at each crossing point shows a divergent behavior when approaching the zero temperature [14–20].

It was interpreted that [21, 22], due to the transformation of the vortex lattice into the vortex glass-like phase in the zero-temperature limit, rare regions of inhomogeneous superconducting (SC) islands (or puddles) gradually emerge in the high field regime. As a result, the quantum Griffiths singularity emerges, which manifests an activated scaling behavior in a limited temperature range. It is believed that [14] such a vortex glass-like phase is rather delicate against the thermal

fluctuation, since in the high-temperature region, thermal fluctuations will smear the inhomogeneity caused by quenched disorder. Thus the rare regions of the SC islands could not exist. In other words, the quantum Griffiths singularity can only be observed in extremely low temperatures, where the impact of quenched disorder overtakes thermal fluctuations. Although it has been pointed out theoretically that [22] the dominant of spin-related pair-breaking effect will lead to a larger energy associated with the formation of the SC puddles, it is still unknown concerning the upper limit of temperature that QGS can survive. Especially, there is no related experimental results on this issue.

In this study, we conducted an in-depth investigation on the field induced superconductor-metal transition in NbN thin films, whose SC critical temperature T_c has been tuned to below 4 K. Systematic variation of the crossing points B_x and the effective critical exponents ν are observed in a finite temperature range. Moreover, the temperature and field dependence of sheet resistance can be described by the activated dynamical scaling in a relatively wide temperature region up to 4.0 K. Our finding indicates that the features of the quantum Griffiths singularity actually can survive at a higher temperature than we have expected previously.

2 Materials and methods

The NbN thin films were deposited using the method of DC reactive magnetron sputtering. The details of the conditions for the film growth have been reported previ-

ously [23]. In the present work, two films (W11 and W6) grown under different chamber pressures were chosen to conduct the following investigations. The thicknesses of the two films were determined by the X-ray reflectivity (XRR) measurements to be 25 and 20 nm, respectively. The films were etched into the line shape with the dimension $10 \times 500 \mu\text{m}^2$ using reactive ion etching (RIE) for the electrical transport measurements.

The electrical transport measurements were performed using a cryostat (Oxford Instruments TeslatronPT cryostat system) with the field of up to 12 T. The applied electric current is $0.5 \mu\text{A}$ during the transport measurements. The magnetic field were applied perpendicular to both the film surface and the direction of electrical current.

3 Results

The sheet resistance R_s as a function of temperature of the two samples are shown in Fig. 1. Under zero field, as shown in Fig. 1(a), clear SC transitions can be seen in the R_s - T curves, with the T_c of 2.5 K and 3.9 K for the samples W11 and W6, respectively. Besides the superconductivity, the magnitude of sheet resistance in the normal state just above T_c , R_N , also reveals a clear different between the two samples: $R_N = 1400$ and 650Ω for W11 and W6, respectively. It is notable that the R_s - T under a high field of 12 T shows a logarithmic temperature dependence in the low temperature region, see Fig. 1(b). This feature is the hallmark of the 2D quantum corrected disordered metal, where weak localization play a crucial role in determining the nature of electrons [18, 24].

In order to investigate the detailed characteristic of

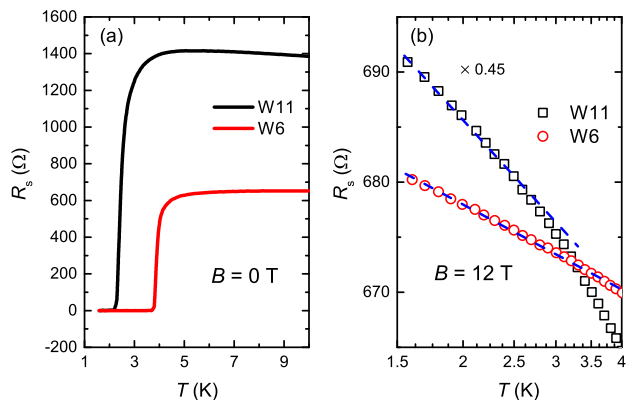


FIG. 1: Temperature dependence of sheet resistance R_s under the magnetic fields of 0 T (a) and 12 T (b) for two samples. The semi logarithmic coordinates is used in (b). The blue dashed lines are visual guides.

this field induce transition from the SC to metallic state, we measured the temperature dependence of R_s under a series of magnetic fields up to 12 T. The data of sample W11 are displayed in Fig. 2. As shown in Fig. 2(a), with the increase of field, the steep descent behavior due the SC transition is suppressed gradually, and eventually turns into a quantum corrected metallic state. By carrying out a matrix inversion of the temperature-swept data, field dependence of R_s can be generated, which is shown in Fig. 2(b). A series and continuum of crossings in the R_s - B curves can be seen, which spreads out over a range of temperatures (1.6-5 K) and magnetic fields. We extracted the positions of the crossing points B_x and showed them in Fig. 2(c) as a function of temperature. Such an evolution of B_x can be simulated using the equation based on the activated scaling [18]

$$B_x(T) = B_c \times [1 - u(\ln \frac{T_0}{T})^{-p}], \quad (1)$$

where B_c is the critical field in the zero-temperature limit, u and p are fitting parameters. The fitting result is presented by the blue solid line in Fig. 2(c).

Similar to the previous reports in other systems [14, 18–20], the R_s - T data in Fig. 2(b) in each small temperature intervals can be analyzed using the conventional power-law scaling

$$R_s(\delta_x, T) = F(\delta_x T^{-1/z\nu}), \quad (2)$$

where $\delta_x = |B - B_x|/B_x$ is the normalized distance from the effective critical field B_x in each small temperature ranges, ν is the correlation-length exponent, z is the dynamical-scaling exponent, and F is the scaling function with $F(0) = 1$. The results of the scaling using Eq. 2 are shown in the Supplementary Material (SM). The obtained critical exponents $z\nu$ as a function of field are shown in Fig. 2(d). With the decrease of temperature, the value of $z\nu$ reveals an upward trend with an increasing steepness. Such a divergent tendency is simulated using the equation based on the activated scaling

$$z\nu = C \times |B - B_c|^{-0.6}, \quad (3)$$

where C is the fitting parameter. The power exponent is set as the value (~ 0.6) used by other groups [14, 20]. As shown by the blue solid line, the experimental data, especially the divergent tendency in the low temperature region, can be well described by Eq. 3.

Theoretically, quantum Griffiths singularity is closely related with an infinite-randomness critical point. Strictly speaking, the quantum SMT governed by such an infinite-randomness fixed point could not be described by the conventional power-law scaling. Recently, the activated dynamical scaling was proposed [18] in the following form

$$R_s(\delta, \ln \frac{T_0}{T}) = \Phi[\delta(\ln \frac{T_0}{T})^{1/\nu\psi}]. \quad (4)$$

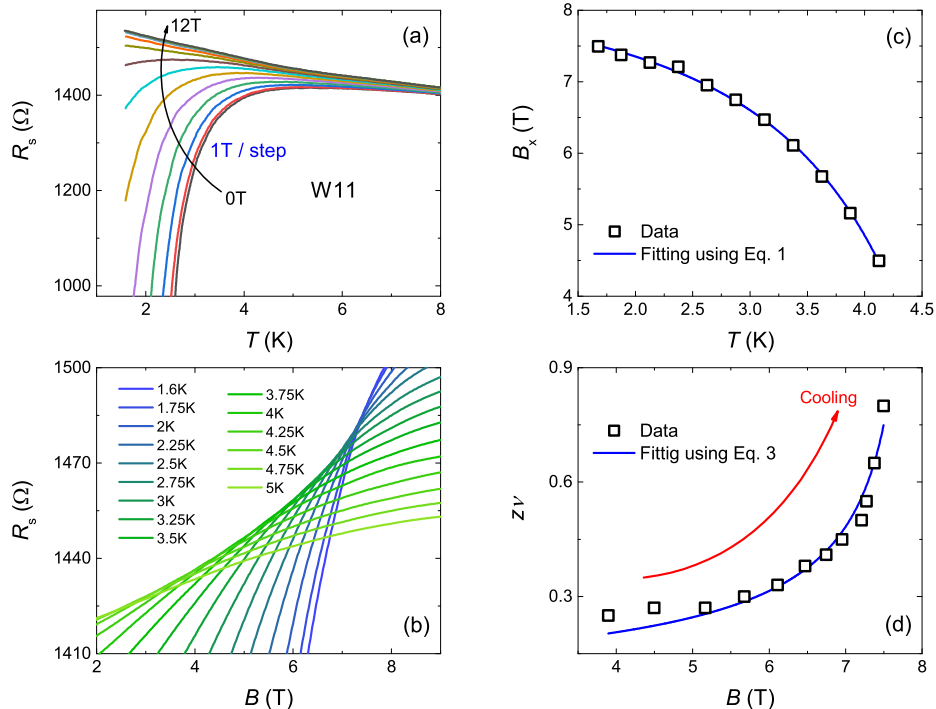


FIG. 2: (a) Temperature dependence of sheet resistance under magnetic fields up to 12 T for sample W11. (b) Field dependence of sheet resistance at temperatures ranging from 1.6 K to 5 K. (c) Crossing points from the magnetoresistance isotherms shown in (b). The blue solid line is a fit to the equation (see text). (d) Field dependence of the critical exponent $z\nu$ obtained from finite size scaling analysis. The blue solid line shows the fitting curve based on the activated scaling law.

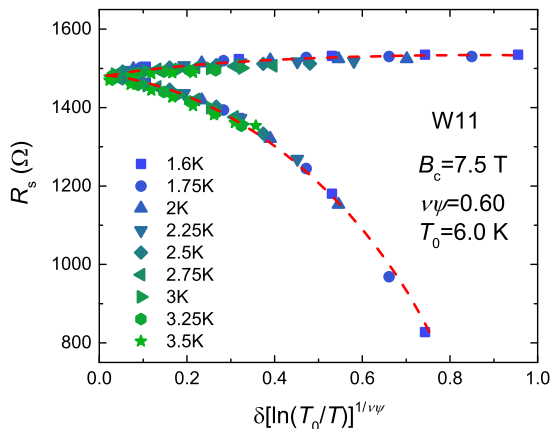


FIG. 3: Sheet resistance as a function of scaling variable $\delta[\ln(T_0/T)]^{1/\nu\psi}$ in the temperature range $1.6 \text{ K} \leq T \leq 3.5 \text{ K}$. The red dashed lines are visual guides.

Here $\delta = |B - B_c|/B_c$ is the normalized distance from the critical field B_c , exponent ψ is the tunneling exponent, and T_0 is a microscopic temperature scale. Φ is the function of the activated dynamical scaling. According to this equation, there is only one single crossing point in

magnetic field, which does not account for the temperature dependence of the crossing fields in the experimental data. In Fig. 3, we show the results of the activated dynamical scaling according to Eq. 4. All the experimental data in the temperature range $1.6 \text{ K} \leq T \leq 3.5 \text{ K}$ collapse into a single curve, indicating the rationality of the activated dynamical scaling in describing our data. From this scaling, the critical exponent $\nu\psi = 0.60$ and critical field $B_c = 7.5 \text{ T}$ were obtained. The value of $\nu\psi$ obtained here is slightly smaller than that reported in InO_x films (~ 0.62) [18].

Sample W6, with a relatively higher T_c and lower R_N , also reveals the field induced SMT, as shown in Fig. 4(a). Similar to that observed in sample W11, the crossing points in the R_s - B curves experience a series of evolution with temperature, which tends to be saturated at above 9 T as the temperature goes towards lower temperatures (see Fig. 4(b)). The values of the crossing fields B_x are recorded in Fig. 4(c), from which the saturated tendency can be seen more clearly. Again the B_x - T data are simulated using Eq. 1 as revealed by the red solid line in Fig. 4(c). The temperature and field dependence of sheet resistance in the temperature range $1.6 \text{ K} \leq T \leq 4.0 \text{ K}$ are analyzed using the activated dynamical scaling, which are shown in Fig. 4(d). The scaling parameters are $B_c = 9.6 \text{ T}$, $\nu\psi = 0.55$, and $T_0 = 9.1 \text{ K}$. These parameters

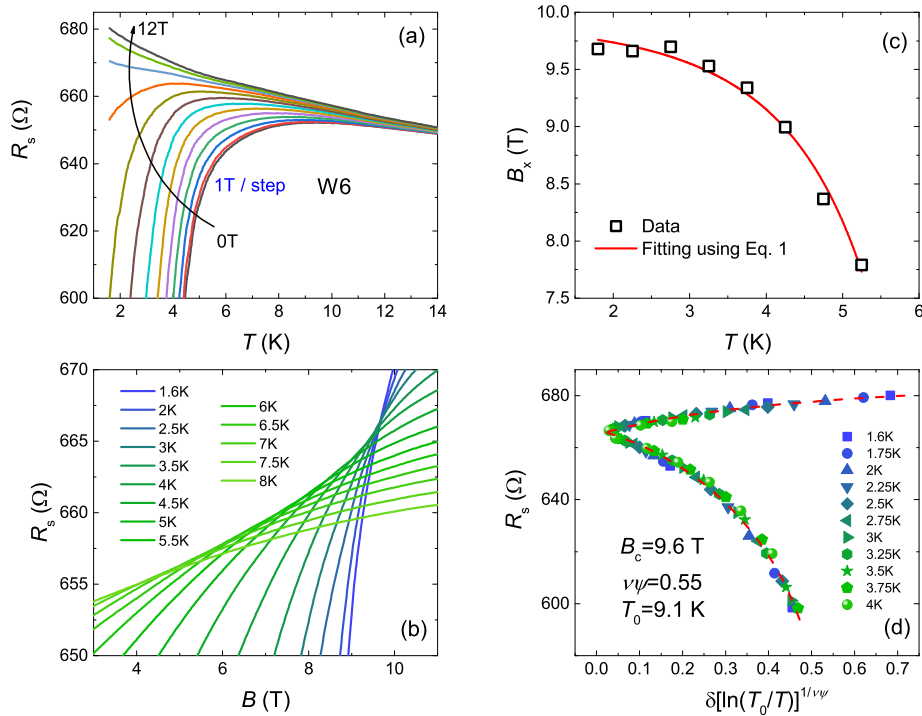


FIG. 4: (a) Temperature dependence of sheet resistance under magnetic fields up to 12 T for sample W6. (b) Field dependence of sheet resistance at temperatures ranging from 1.6 K to 8 K. (c) Crossing points from the magnetoresistance isotherms shown in (b). The red solid line is a fit to the equation (see text). (d) Sheet resistance as a function of scaling variable $\delta[\ln(T_0/T)]^{1/\nu\psi}$ in the temperature range $1.6 \text{ K} \leq T \leq 4 \text{ K}$. The red dashed lines are visual guides.

TABLE I: Important parameters of the two samples.

Name	T_c (K)	R_N (Ω)	B_c (T)	$\nu\psi$	T_0 (K)
W11	2.5	1400	7.50	0.60	6.0
W6	3.9	650	9.60	0.55	9.1

of the two samples are summarized in Table 1 to have a comparison.

4 Discussion

The adjustability in a large range of the physical properties of NbN films [23, 25, 26] provides convenience to broaden the extension of ground state in investigating the quantum phenomena, like quantum Griffiths singularity in field induced SMT. In this work, the sheet resistance in the normal state is tuned from 1400 Ω to 650 Ω . Our results suggest that, the quantum Griffiths singularity can be observed in the system with R_N being suppressed to half. In the case of PdTe₂ films [20], the features of quantum Griffiths singularity has disappeared under perpendicular field when R_N is reduced to below 200 Ω by increasing the film thickness. Finding and determining

the critical point of where QGS disappears is of great significance for revealing the essence of this quantum phenomenon. Based on the NbN film, we can systematically adjust its normal state resistance without changing the film thickness, so that the boundary of the QGS state can be accurately determined without changing other factors. This will be the next step of our work.

Another important issue worth our attention is the temperature range where QGS occurs. Based on general understanding [14], QGS is rather delicate against the thermal fluctuation, since the inhomogeneity caused by quenched disorder can be smeared by the thermal fluctuations in the high-temperature region. In this case, the rare regions of the SC islands (puddles) could hardly survive. Indeed, previously the signatures of QGS were typically detected in the extremely low temperatures. In our work, however, it is found that the activated dynamical scaling can describe the electrical transport data in the temperature range $1.6 \text{ K} \leq T \leq 3.5 \text{ K}$ (see Fig. 3) or $1.6 \text{ K} \leq T \leq 4.0 \text{ K}$ (see Fig. 4(d)).

Theoretically, the size, distance, and concentration of the SC puddles are important parameters in controlling the performance of the QGS [22]. These factors determine the coupling strength between optimal puddles. Moreover, in the magnetic field induced SMT, the modes of coupling between the applied field and the SC state

can also play an important role, which may give a different microscopic physics responsible for the emergence of the puddle state. It was pointed out that [22], compared with the case that the field couples primarily to the electron's orbital motion, the coupling to the electron spin (Zeeman coupling) in the absence of spin-orbit coupling can lead to a larger energy associated with the formation of puddles. In this case, the puddle state should be more robust. In our previous work [23], we have uncovered a clear Pauli paramagnetic effect in the present NbN system, which emphasizes the significant influence of the coupling between the magnetic field and spin degree of freedom. It seems that this is the most probable reason why we have observed such a robust QGS state in NbN films. We expect to observe similar behaviors in more systems with a strong Pauli paramagnetic effect in the future.

5 Conclusions

In summary, we studied the field induced superconductor-metal transition in the NbN thin films. The quantum Griffiths singularity, in terms of the systematical evolution of the crossing point B_x in the R_s - B curves and the applicability of the activated scaling analysis to the transport data, was observed in two samples with different T_c and R_N . Significantly, activated scaling can be valid in the temperature range as high as 1.6 K – 4.0 K, revealing the robustness of the QGS in the present system. Our analysis indicates that the strong Pauli paramagnetic effect in NbN films plays a key role in enhancing the stability of the puddle state, which is the precondition for the formation of QGS.

This work is supported by the National Natural Science Foundation of China (No. 92065116), the Shanghai Technology Innovation Action Plan Integrated Circuit Technology Support Program (No. 22DZ1100200), and the Key-Area Research and Development Program of Guangdong Province, China (No. 2020B0303030002). The authors would like to thank all the staff at the Superconducting Electronics Facility (SELF) for their assistance.

* w.li@fudan.edu.cn

† mugang@mail.sim.ac.cn

‡ zrlin@mail.sim.ac.cn

- [1] M. Imada, A. Fujimori, and Y. Tokura, *Rev. Mod. Phys.* **70**, 1039 (1998).
 [2] V. F. Gantmakher and V. T. Dolgoplov, *Physics-Usppekhi* **53**, 1 (2010).

- [3] N. Marković, C. Christiansen, and A. M. Goldman, *Phys. Rev. Lett.* **81**, 5217 (1998).
 [4] A. Yazdani and A. Kapitulnik, *Phys. Rev. Lett.* **74**, 3037 (1995).
 [5] J. Biscaras, N. Bergeal, S. Hurand, C. Feuillet-Palma, A. Rastogi, R. C. Budhani, M. Grilli, S. Caprara, and J. Lesueur, *Nat. Mater.* **12**, 542 (2013).
 [6] Y. Sun, H. Xiao, M. Zhang, Z. Xue, Y. Mei, X. Xie, T. Hu, Z. Di, and X. Wang, *Nat. Commun.* **9**, 2159 (2018).
 [7] R. Schneider, A. G. Zaitsev, D. Fuchs, and H. v. Löhneysen, *Phys. Rev. Lett.* **108**, 257003 (2012).
 [8] T. Wang, A. Yu, Y. Liu, G. Gu, W. Peng, Z. Di, D. Jiang, and G. Mu, *Phys. Rev. B* **106**, 104509 (2022).
 [9] A. T. Bollinger, G. Dubuis, J. Yoon, D. Pavuna, J. Misewich, and I. Božović, *Nature* **365**, 458 (2011).
 [10] X. Leng, J. Garcia-Barriocanal, S. Bose, Y. Lee, and A. M. Goldman, *Phys. Rev. Lett.* **107**, 027001 (2011).
 [11] M. Liao, Y. Zhu, J. Zhang, R. Zhong, J. Schneeloch, G. Gu, K. Jiang, D. Zhang, X. Ma, and Q. K. Xue, *Nano Lett.* **18**, 5660 (2018).
 [12] F. Wang, J. Biscaras, A. Erb, and A. Shukla, *Nat. Commun.* **12**, 2926 (2021).
 [13] Y. Yu, L. Ma, P. Cai, R. Zhong, C. Ye, J. Shen, G. Gu, X. H. Chen, and Y. Zhang, *Nature* **575**, 156 (2019).
 [14] Y. Xing, H.-M. Zhang, H.-L. Fu, H. Liu, Y. Sun, J.-P. Peng, F. Wang, X. Lin, X.-C. Ma, Q.-K. Xue, et al., *Science* **350**, 542 (2015).
 [15] S. Shen, Y. Xing, P. Wang, H. Liu, H. Fu, Y. Zhang, L. He, X. C. Xie, X. Lin, J. Nie, et al., *Phys. Rev. B* **94**, 144517 (2016).
 [16] Y. Xing, K. Zhao, P. Shan, F. Zheng, Y. Zhang, H. Fu, Y. Liu, M. Tian, C. Xi, H. Liu, et al., *Nano Letters* **17**, 6802 (2017).
 [17] Y. Saito, T. Nojima, and Y. Iwasa, *Nat. Commun.* **9**, 778 (2018).
 [18] N. A. Lewellyn, I. M. Percher, J. Nelson, J. Garcia-Barriocanal, I. Volotsenko, A. Frydman, T. Vojta, and A. M. Goldman, *Phys. Rev. B* **99**, 054515 (2019).
 [19] X. Han, Y. Wu, H. Xiao, M. Zhang, M. Gao, Y. Liu, J. Wang, T. Hu, X. Xie, and Z. Di, *Adv. Sci.* **7**, 1902849 (2020).
 [20] Y. Liu, S. Qi, J. Fang, J. Sun, C. Liu, Y. Liu, J. Qi, Y. Xing, H. Liu, X. Lin, et al., *Phys. Rev. Lett.* **127**, 137001 (2021).
 [21] T. Vojta, *J. Low Temp. Phys.* **161**, 299 (2010).
 [22] B. Spivak, P. Oretov, and S. A. Kivelson, *Phys. Rev. B* **77**, 214523 (2008).
 [23] X. Wang, L. Wang, Y. Liu, W. Gao, Y. Wu, Z. Xu, H. Jin, L. Zhang, W. Peng, Z. Wang, et al., unpublished (2022).
 [24] B. Kramer and A. MacKinnon, *Rep. Prog. Phys.* **56**, 1469 (1993).
 [25] G. Oya and Y. Onodera, *J. Appl. Phys.* **45**, 1389 (1974).
 [26] Z. Wang, A. Kawakami, Y. Uzawa, and B. Komiyama, *J. Appl. Phys.* **79**, 7837 (1996).